Metallomics

Influence of reducing agents on the cytotoxic activity of platinum(IV) complexes: induction of G2/M arrest, apoptosis and oxidative stress in A2780 and cisplatin resistant A2780cis cell lines

Journal:	*Metallomics*
Manuscript ID:	MT-ART-05-2015-000116.R1
Article Type:	Paper
Date Submitted by the Author:	03-Jun-2015

Complete List of Authors:	Pichler, Verena; University of Vienna, Goeschl, Simone; University of Vienna, Institute of Inorganic Chemistry Schreiber-Brynzak, Ekaterina; University of Vienna, Institute of Inorganic Chemistry Jakupec, Michael; University of Vienna, Institute of Inorganic Chemistry Galanski, Markus; University of Vienna, Institute of Inorganic Chemistry Keppler, Bernhard; University of Vienna, Institute of Inorganic Chemistry

Influence of reducing agents on the cytotoxic activity of platinum(IV) complexes: induction of G_2/M arrest, apoptosis and oxidative stress in A2780 and cisplatin resistant A2780cis cell lines

Verena Pichler,[†,§] Simone Göschl,[†] Ekaterina Schreiber-Brynzak,[†] Michael A. Jakupec,[*,†] Markus Galanski,[†] Bernhard K. Keppler[†,§]

† University of Vienna, Faculty of Chemistry, Institute of Inorganic Chemistry, Waehringer Strasse 42, 1090 Vienna, Austria

§ University of Vienna, Research Platform "Translational Cancer Therapy Research", Waehringer Strasse 42, 1090 Vienna, Austria

*Corresponding author. Tel. +43 1 4277 52610. E-mail address: michael.jakupec@univie.ac.at (M. A. Jakupec).

Abbreviations: AA = ascorbic acid; AV = annexin V; casp 9 = caspase 9; DNA = deoxyribonucleic acid; FBS = fetal bovine serum, GSH = glutathione; HSF = hypotonic fluorochrome solutions; ICP-MS = inductively coupled plasma mass spectrometry; MEM = minimum essential medium; MTT = 3-(4,5-dimethylthiazol-2-yl)-2,5-diphenyltetrazolium bromide; NAC = N-acetyl cysteine; NMR = nuclear magnetic resonance; oc = open circular; PARP = poly(ADP-ribose)polymerase; PBS = Dulbecco's phosphate-buffered saline, PI = propidium iodide; RF = resistance factor; PVDF = polyvinylidene difluoride, RIPA = radioimmunoprecipitation assay buffer, ROS = reactive oxygen species; RPMI = Roswell Park Memorial Institute medium; sc = supercoiled; SD = standard deviation; SDS-PAGE = sodium dodecyl sulfate polyacrylamide gel electrophoresis.

Abstract

The concept of Pt^{IV} prodrug design is one advanced strategy to increase the selectivity for cancer cells and to reduce systemic toxicity in comparison to established platinum-based chemotherapy. Pt^{IV} complexes are thought to be activated by reduction *via* physiological reductants, such as ascorbic acid or glutathione. Nevertheless, only few investigations on the link between reduction rate, which is influenced by the reductant, and the ligand sphere of the Pt^{IV} metal centre have been performed so far. Herein, we investigated a set of Pt^{IV} compounds with varying rate of reduction with respect to their cytotoxicity and drug accumulation in A2780 and A2780cis ovarian cancer cell lines, their influence on the cell cycle, efficiency of triggering apoptosis, and ability to interfere with plasmid DNA (pUC19). Effects caused by Pt^{IV} compounds were compared without or with extracellularly added ascorbic acid and glutathione (or its precursor N-acetylcysteine) to gain understanding of the impact of increased levels of reductant on the activity of such complexes. Our results demonstrate that reduction is required prior to plasmid interaction. Furthermore, the rate of reduction is crucial for the efficiency of this set of Pt^{IV} compounds. The substances that are reduced least likely showed similar performances, whereas the fastest reducing substance was negatively affected by an increased extracellular level of reducing agents, with reduced cytotoxicity and lower efficiency in inducing apoptosis and G_2/M arrest. These results confirm the connection between reduction and activity, and prove the strong impact of the reduction site on the activity of Pt^{IV} complexes.

1. Introduction

Platinum(IV) complexes have the potential of being the next generation of metal-containing anticancer agents in clinical use, following the well-established Pt^{II} drugs cisplatin, carboplatin and oxaliplatin. The most prominent representative, satraplatin, was undergoing different clinical phase I, II, and III trials, most of them finished or stopped, however [1,2]. It is widely accepted that Pt^{IV} complexes act as prodrugs [3], as they undergo reduction in the hypoxic region of solid tumours, thereby releasing the corresponding active Pt^{II} species (activation by reduction). Nevertheless, the main reducing agent in the blood stream or at the tumour site is currently unknown; and whether the reduction process occurs intra- or extracellularly is still under debate. Identified contributors to the reduction of Pt^{IV} are small molecules such as glutathione (GSH) or ascorbic acid (AA), which are available in the blood stream as well as inside the cell, but also high molecular weight agents, such as metallothioneins, myoglobin and haemoglobin, are potential reductants [4,5]. The physicochemical parameters most decisive for where and whether the prodrug is reduced are the reduction potential [6,7] and the rate of reduction [8–12]. These parameters are strongly influenced by the ligand sphere of the central metal ion. As Pt^{IV} complexes are octahedrally configured, and therefore have six binding sites for ligands, there are numerous possibilities for controlling the reduction parameters. Recently, an increasing number of Pt^{IV} compounds were synthesized with mixed axial ligands [13–15], opening up new, mostly unexplored ligand spheres. Compared with the well-known symmetrically dicarboxylated complexes (especially satraplatin), these unsymmetrically substituted complexes offer, apart from a different solubility and lipophilicity, a distinctly diverging rate of reduction [8,9]. The effects of the altered ligand sphere on the biological behaviour have scarcely been investigated so far. Nevertheless, results of symmetrically dicarboxylated Pt^{IV} complexes allow some insights and a comparison with regard to the mode of action of unsymmetrically substituted compounds.

Although these complexes are considered inert and are therefore expected not to bind to DNA without prior reduction, interactions with plasmids after 24 h were measured for Pt^{IV}-bis(monoglutarate) [16], and binding of enPt(OCOOCH3)$_4$ to 5'-GMP could be detected in ^{1}H-NMR experiments [17]. However, reactions were far too slow to be relevant for the mode of action. Although platinum drugs face a multitude of reactants on their way to the cancerous cells, it is proven that a measurable amount of platinum reaches its main target, the DNA. Kelland and coworkers compared the intracellular amount of platinum and the traces of platinum bound to DNA. In the case of the most important representative of Pt^{IV} compounds, satraplatin, about 10% of the detected intracellular Pt was found in the DNA fraction of different ovarian carcinoma cell lines [18]. Furthermore, satraplatin treatment has a significant impact on the cell cycle, as it induces a strong G_2/M arrest and finally apoptosis in different colorectal cancer [19] and in L1210 murine leukaemia cells [20]. Although it is well known that cisplatin induces apoptosis mainly via the mitochondrial apoptosis pathway (intrinsic pathway) [21], only a small amount of investigations have been published for Pt^{IV} complexes so far. Finally, satraplatin resistance was described to be caused by an increased tolerance to Pt-DNA adducts in CH1 cells and elevated GSH levels in SK-OV-3 cells [18].

Herein, we investigate four PtIV complexes [9] and satraplatin as a reference compound (Fig. 1) on their altered behaviour in the presence of cellular available reducing agents ascorbic acid (AA), glutathione (GSH), and its precursor N-acetylcysteine (NAC). The platinum compounds are comparable in their stability in aqueous solutions, and result in analogous metabolites with similar rate of aquation. However, they significantly differ in their lipophilicity, reduction potential and rate of reduction and for that reason are highly suitable as model complexes for investigating the biological differences triggered by the afore-mentioned reduction parameters.

The impact of co-incubation of Pt^{IV} complexes with the most common cellular available antioxidants on their cytotoxic activity, cellular accumulation, cell cycle disturbance, apoptosis and plasmid interaction ability were elaborated in *in vitro* experiments. The efficiency of AA and GSH in reducing the investigated Pt^{IV} complexes was elucidated, in order to correlate physicochemical with biological parameters. In parallel, the corresponding Pt^{II} substrate (Fig. 1, compound **5**), which is the putative main metabolite was additionally tested for its IC_{50} value in the absence and presence of NAC and GSH (Pt^{II} : S-containing reductant = 1 : 2) for comparison with IC_{50} values achieved during co-incubation experiments of Pt^{IV} complexes with these reductants.

PLEASE INSERT FIGURE 1 HERE

Figure 1: Chemical structures of investigated complexes **1-5** and reference compound satraplatin.

2. Results and Discussion

2.1. Rate of reduction

The rate of reduction is influencing the time frame within which the Pt^{IV} species should reach its target. Since Pt^{IV} compounds act as prodrugs, reduction is indispensable for the activation of these complexes, as Pt^{IV} complexes are kinetically inert with a very slow ligand exchange rate compared to their Pt^{II} analogues [22].

In order to understand the difference in the interaction of Pt^{IV} compounds featuring *trans*-OH, *trans*-OAc ligands or the mixture thereof (unsymmetric compound with one OH opposing an OAc ligand) with physiologically relevant reducing agents (AA and GSH), compounds **1**–**4**, and

satraplatin were incubated with a two-fold excess of the reducing agent in a phosphate buffered D_2O solution, and time dependent ^{1}H-NMR measurements were performed over a period of at least 24 h at 25 °C (Fig. 2). These conditions were chosen for a better comparison with the rates of reduction of previously published *N*,*N*-dimethylethane-1,2-diamine Pt^{IV} analogues. In this context, it is worth mentioning that literature data are quite inconsistent with regard to experimental conditions, ranging from 2- to 25-fold excess of reducing agent with temperatures between r.t. and 37 °C [9,10,23].

The rate or reduction of octahedrally configured Pt^{IV} complexes with a *cis*,*trans*,*cis*-$PtN_2(OR)_2Cl_2$ ligand sphere, is significantly influenced by the type of substituent. Comparing complexes with the *N*,*N*-diethylethane-1,2-diamine chelating ligand, the dihydroxido compound **1** (R = H) is reduced least likely (reduction half time > 15 h) and the dicarboxylated one **3** (R = COR) most likely (reduction half time approx. 15 min). The reduction half time of compound **2**, featuring mixed axial ligands, is intermediate between those of the symmetric derivatives (reduction half time approx. 5 h). These results are in very good agreement with previously published and structurally comparable platinum(IV) complexes with an equatorial chelating *N*,*N*-dimethylethane-1,2-diamine ligand [9]. Links between axial ligands and reduction were already reported in the literature, though not always in a comparable order, as Gibson and coworkers reported the reverse effect for compounds with a *cis*,*trans*,*cis*-$N_2(OR^1)_2(OR^2)_2$ ligand sphere [8].

The reduction of satraplatin and **4** is not proceeding as fast as for **3** despite the fact that all three complexes have the same axial ligands coordinated. As the only structural difference between these substances is the chelating moiety, the reason for the varying rates must be connected to the substituents at one of the chelating nitrogens (R^1R^2-N-CH_2-CH_2-NH_2). The rate of reduction of the dicarboxylated complexes increases in the following order: satraplatin ($R_1 = R_2 = H$) < **4**

(R_1 = cyclohexyl; R_2 = H) < **3** (R_1 = R_2 = ethyl), concluding that derivatisation at this position leads to an additional destabilization of the complexes with regard to reduction. We demonstrate here that a substitution at the nitrogen of the chelating equatorial position has a strong influence on the rate of reduction, too.

PLEASE INSERT FIGURE 2 HERE

Figure 2: ^{1}H-NMR measurements of the reduction of platinum complexes **1**–**4** and reference compound satraplatin with selected reducing agents. Incubation experiments were performed with a 1:2 ratio of complex to reductant at 25 °C in phosphate buffered D_2O solution (pD = 7.51). **A**: Pt^{IV} complexes were incubated with AA; **B**: Pt^{IV} complexes were incubated with GSH; compounds **1** (■), **2** (▲), **3** (□), **4** (●), and satraplatin (◆).

Furthermore, experiments showed that the type of reducing agent has a dramatic impact on the effectiveness of Pt^{IV} complexes. Ascorbic acid was distinctly more potent than sulphur containing reducing agents, such as glutathione.

Summarizing, ^{1}H-NMR studies of investigated complexes **1**, **2**, **3**, **4**, and satraplatin are in very good accordance with previously published results, showing an increasing reduction half time in the following order for incubation with AA: **3** << **2** < **4** < satraplatin << **1**. The rate of reduction is highly influenced by structural characteristics of the platinum complexes, such as the type of axial ligand as well as the bulkiness of the residues of the chelating ethan-1,2-diamine moiety. Glutathione is not as effective in reducing the investigated compounds as ascorbic acid. In presence of GSH only **3** is reduced within a biologically relevant time range. The increasing

order is as follows: **3** << **4** < satraplatin ≤ **2** ≤ **1**. Nevertheless, these complexes are perfect model complexes for investigating the connection between reduction rate and antiproliferative activity, as they are structurally related, but strikingly different in their redox behaviour.

2.2. Plasmid interaction studies

The ability of damaging DNA is essential for a potent platinum drug in respect of the postulated mode of action. Hence, Pt^{II} complexes have been extensively studied with respect to their binding kinetics, and interference with DNA [24–26]. Pt^{IV} drugs do not possess sufficiently fast binding and ligand exchange kinetics, and therefore reduction is mandatory (activation by reduction) prior to DNA binding [17]. So far, only a small number of publications have dealt with the successive processes of reduction and target binding. Gibson and coworkers as well as Banfic *et al.* are dealing, e.g., with the reduction behaviour in cancer cell lysates [27,28]. Furthermore, Steinborn *et al.* performed some plasmid interaction studies in the presence of ascorbic acid under very harsh conditions (24 h at 37 °C, with up to a 1:1 ratio of nucleotides:Pt^{IV} complex), reasoning that this leads to strong DNA fragmentation and degradation [29].

Nevertheless, changes in the electrophoretic mobility of the supercoiled (sc) and the open circular plasmid (oc) form in an agarose gel is an easy and versatile method to study DNA interactions in cell-free settings. Especially as side reactions, which may deactivate the platinum prodrug, are excluded from these experiments. Therefore, a mixture of the investigated Pt^{IV} complexes and the reducing agents (GSH or AA, ratio 1:2) were incubated with pUC19 at 37 °C (Fig. 3) to get a better understanding of the influence of the reduction rate on subsequent untwisting of the supercoiled plasmid form. Prior to co-incubation experiments, the platinum(IV)

compounds as well as the reducing agents alone were incubated with pUC19, to check whether these substances can cause untwisting of the sc plasmid form (Fig. S1; ESI). As anticipated, without reduction, hardly any of the investigated complexes showed signs of affecting the supercoiled form of pUC19 within a 6 h time frame. The only exception was substance **4** causing a minor retardation of the sc configuration of the plasmid after 6 h. Furthermore, it was proven that the applied reducing agents are not interfering with the plasmid.

Co-incubation of the complexes with a two-fold excess of ascorbic acid lead to untwisting of the supercoiled configuration to the open circular one in a time and reduction rate dependent manner. **1** and satraplatin started to interact with the pUC19 plasmid after about 4 h, whereas the plasmid incubated with **2** was already converted completely into the oc DNA form at this time point. The complexes reacting fastest with the plasmid under these conditions were **3** and **4**; these two are furthermore the only complexes which show effects on the plasmid configuration after around 4 h in the GSH co-incubation experiments. The rate of reduction observed during ^{1}H-NMR experiments was strongly reflected during the plasmid binding studies, as the fast reducing complex **3** was interacting already after 1 h with pUC19 DNA in the presence of AA and after 4 h in the presence of GSH, while the slowly reducing compounds **1** and satraplatin just show minor interactions after 4 h in AA co-incubation experiments and no effect upon co-incubation with GSH. Therefore, plasmid interaction studies showed that reduction is essential for the efficiency of Pt^{IV} prodrugs. Our experiments proved that a consecutive process of (i) reducing the complex, (ii) releasing a Pt^{II} species and (iii) subsequent interfering with DNA has to occur, before cells are significantly affected by the substance, as no interaction takes place, when platinum is still in the oxidation state IV.

PLEASE INSERT FIGURE 3 HERE

Figure 3: Plasmid interaction studies. pUC19 was incubated with indicated Pt^{IV} compounds (50 µM) and the respective reducing agents (100 µM) for 15 min, 1 h, 2 h, 4 h, and 6 h at 37 °C in a TE buffer system. Changes in the plasmid configuration were measured by agarose gel electrophoresis mobility shift assay.

2.3. Cytotoxic activity in ovarian carcinoma cell lines

The investigated Pt^{IV} complexes were tested with respect to their cytotoxic activity in the cisplatin sensitive and resistant human ovarian carcinoma cell lines A2780 and A2780cis, respectively. The resistance in A2780cis cells is caused by an increased GSH level, enhanced DNA repair and/or tolerance [30], and is therefore the cell line of choice to study effects caused by an increased level of the reductant GSH.

Table 1: Cytotoxic activity in presence or absence of AA, NAC, or GSH of Pt compounds **1**–**5** and reference compound satraplatin measured by means of the MTT assay in A2780 and A2780cis ovarian carcinoma cell lines after an incubation time of 96 h.

	IC_{50} [µM][a]				
Cmp	**A2780**	***p***	**A2780cis**	***p***	**RF**
1	6.1 ± 0.8		47 ± 8		7.7
1 + AA	5.2 ± 2.2		64 ± 4	*	12.3
1 + NAC	12 ± 1	**	60 ± 19		5.0

2	2.7 ± 0.2		17 ± 2		6.3
2 + AA	5.5 ± 1.8	*	23 ± 6		4.3
2 + NAC	6.0 ± 2.6	**	26 ± 9		4.4
3	1.7 ± 0.1		6.9 ± 1.9		4.1
3 + AA	4.2 ± 0.4	*	22 ± 3	*	5.2
3 + NAC	17 ± 1	**	55 ± 17	**	3.2
4	1.3 ± 0.3		7.4 ± 0.7		5.7
4 + AA	2.0 ± 0.4		7.4 ± 1.8		3.7
4 + NAC	2.0 ± 0.7		12 ± 1		6.0
5	4.5 ± 0.3		17 ± 3		3.8
5 + NAC	4.4 ± 1.2		17 ± 2		3.9
5 + GSH	4.4 ± 1.6		18 ± 2		4.1
Satraplatin	0.38 ± 0.03		2.6 ± 0.3		6.8
Satraplatin + AA	0.33 ± 0.08		2.4 ± 0.6		7.3
Satraplatin + NAC	0.83 ± 0.33		3.1 ± 0.3		3.7
cisplatin[b]	0.70 ± 0.02		3.7 ± 0.3		5.3

[a]Values are given as means ± SD from at least three independent experiments performed in triplicate. Statistical significance was calculated for compound alone compared to compound in presence of AA or NAC (* $p < 0.05$; ** $p < 0.01$).

[b]Values taken from Reference [31].

In A2780 cancer cells, all complexes showed IC_{50} values in the low micromolar range. Resistance factors in the corresponding cisplatin resistant cell line range from 3.8 to 7.7, which is well comparable to satraplatin and cisplatin. In further experiments, compounds were added to the cells for 96 h in presence of ascorbic acid (constant concentration of 25 μM) or N-acetylcysteine (NAC, 150 μM in A2780, 200 μM in A2780cis) (Table 1; Fig. S2; ESI). Prior to the co-incubation experiments, the maximum non-cytotoxic concentration of NAC and AA were determined to exclude direct effects caused by the reducing reagents (Fig. S3, ESI).

IC_{50} values of complexes **1**, **4**, and satraplatin were not altered or only slightly influenced by co-incubation with AA (ranging from 1- to 1.9-fold increase) and NAC (ranging from 1.3- to 2-fold increase) in both cell lines. Compound **2** experienced a significant decrease of cytotoxic activity in the presence of AA or NAC up to 2.2-fold in A2780 cells. These results show that very fast reduction rates (< ~15 min) are required to monitor biologically relevant effects caused by reduction *in vitro* and confirm the high impact of the redox behaviour on cytotoxicity. Therefore, complex **3,** with a reduction half time of about 15 min at 25 °C, experienced the most significant shift of the concentration-effect curve to higher concentrations. In detail, a 2.5-fold increase (*) was observed for the fast reducing complex **3** in A2780 (1.7 ± 0.1 μM vs. 4.2 ± 0.4 μM) and an about 3.2-fold increase (*) in A2780cis cells (6.9 ± 1.9 μM vs. 22 ± 3 μM). The deactivation effect was more pronounced for the applied reductant NAC than for AA. The IC_{50} values were changed around 9.9-fold (**) in A2780 (1.7 ± 0.1 μM vs. 17 ± 1 μM) and about 8-fold (**) in A2780cis cells (6.9 ± 1.9 μM vs. 55 ± 17 μM) for **3** co-incubated with NAC.

The cytotoxic activity achieved by co-incubation experiments with **3** and AA corresponds very well to the IC_{50} value of the platinum(II) complex dichlorido(*N*,*N*-diethylethane-1,2-diamine)platinum(II) (**5**) (Table 1), consistent with the expectation that mainly this Pt^{II} species is

released during reduction. As platinum complexes are preferably binding to sulphur containing biomolecules due to the HSAB principle, the additional deactivation observed during NAC co-incubation may be caused by subsequent binding to NAC after the reduction process. For that reason, the Pt^{II} species **5** was then incubated with NAC and GSH in 1:2 ratio, which had no impact on the concentration-effect curves. Hence, an additional deactivation due to coordination of the Pt^{II} species by the sulphur atom of NAC or GSH could not be proven. Basically, our results illustrate that extracellular reduction lead to deactivation of Pt^{IV} complexes with a fast reduction rate.

2.4. Cellular drug accumulation

In order to understand if there is a correlation between cytotoxic activity and cellular accumulation of the investigated complexes, the cellular platinum content was measured by ICP-MS after 2 h of incubation. Obviously, dicarboxylated complexes **3** and **4** were most effectively accumulated in A2780 cells, followed by satraplatin and complex **2**, with compound **1** being accumulated the least (Fig. 4). More precisely, dicarboxylated Pt^{IV} compounds were accumulated by the cells most efficiently with a platinum content of up to 122 fg/cell, whereas one or more free hydroxido groups were highly unfavourable, resulting in cellular platinum concentrations at the detection limit (around 4–5 fg/cell). The platinum accumulation in the resistant A2780cis cell line was generally lower (around 1.7–2.8-fold decreased) than in sensitive A2780 cancer cells, demonstrating that reduced drug accumulation is part of the platinum resistance mechanism in this cisplatin sensitive cell line. Furthermore, as accumulation levels of the fast reducing compound **3** in the co-incubation experiments with AA, and especially NAC, dropped significantly to nearly the level of A2780cis cells, the contribution of increased levels of reductants decreasing drug accumulation is evident.

PLEASE INSERT FIGURE 4 HERE

Figure 4: Accumulation of Pt^{IV} complexes **1**–**4** and satraplatin, as well as complex **3** co-incubated with AA or NAC in A2780 and A2780cis cells measured by ICP-MS. Cells were treated with 50 µM test compound or 50 µM test compound plus 100 µM reducing agent continuously for 2 h at 37 °C. Values are given as means ± SD from at least three independent experiments performed in triplicate (* $p < 0.05$; ** $p < 0.01$).

Thus, increased extracellular levels of reducing agents can be part of platinum resistance mechanisms, and it demonstrates that the site of reduction is crucial for obtaining the desired effects. Drug accumulation is correlating with the previously published lipophilicity [9] and the cytotoxic activity of the complexes (Fig. 5). However, this correlation is only roughly linear, especially as compounds **3** and **4** are taken up more efficiently than satraplatin, although satraplatin is about 3 times more active and has the highest lipophilicity.

PLEASE INSERT FIGURE 5 HERE

Figure 5: Correlation of drug accumulation vs. lipophilicity (left, measured by RP-HPLC, data taken from [9]) and correlation of drug accumulation vs. IC_{50} values (right) in A2780 and A2780cis cells; compounds **1** (■; □), **2** (●; ○), **3** (+; ⊞), **4** (◆; ◇), and satraplatin (▲; △).

Thus, it seems to be true that the released Pt^{II} species are less effectively accumulated compared to their Pt^{IV} congener, for this set of complexes. No influence of the applied reductant (AA vs. NAC) on platinum accumulation was observed as similar platinum levels were measured during co-incubations. In comparison, the results from the MTT co-incubation experiments showed that the presence of sulphur-containing reductants, such as NAC, is more effective in reducing the activity of the complexes than reductants without sulphur (AA). A major contribution to deactivation upon reduction is associated with reduced drug accumulation. However, the reason for the additional deactivation generated by reduction with NAC could not be clarified.

2.5. Analysis of cell cycle distribution

With the aim of gaining a deeper insight into the mode of action, flow cytometric analysis of cell cycle distribution was performed in A2780 and A2780cis cells exposed to four concentrations (around 10 × IC_{50}, 5 × IC_{50}, IC_{50} and 0.1 × IC_{50}) for 24 h and 48 h. The complexes showed moderate effects on the cell cycle after 24 h but significant effects after 48 h in both cell lines.

In A2780 cells, the distribution of the cell cycle phases tended to an increased S phase fraction after 24 h (control: 30%; **1**: 34%; **2**: 37%; **3**: 36%; **4**: 50%; and satraplatin: 41%) with a slightly increased G_2/M phase for complexes **1**–**3** and a decrease of the G_1 phase for all complexes at the highest concentration (~10 × IC_{50}; ESI Fig. S4, S6, S8, S10, and S11). A similar concentration led to pronounced G_2/M phase arrest of 56–78% after 48 h, compared to 25% in the control (Fig. 6). Thereby, the G_1 phase is strongly reduced, whereas the S phase remains more stable. A2780cis cells are less or not affected by the compounds after 24 h (ESI Fig. S4, S6, S8, S10, and S11). Only compound **1** induces an S phase arrest (control 31% vs. 45%) when concentrations of ≥ 100 μM are applied. Nevertheless, after 48 h the impact on the cell cycle

becomes obvious, as for compound **3** and satraplatin an increased S phase and for complexes **1**, **2,** and **4** an increased G_2/M phase fraction was detected. However, the arrest was abrogated at the highest concentration of compound **2**, **4**, and satraplatin, accompanied by an abundance of apoptotic cells.

PLEASE INSERT FIGURE 6 HERE

Figure 6: Impact of platinum compounds **1**, **2**, **4**, and reference compound satraplatin on cell cycle distribution. PI staining and flow cytometry analyses were performed in A2780 and A2780cis cells after 48 h of exposure to the respective complex at the indicated concentrations. Mean percentages ± standard deviations of cells in G_0/G_1, S, and G_2/M phase of the cell cycle are shown (* $p < 0.05$; ** $p < 0.01$; n = 3).

The observed effects on the cell cycle distribution were not substantially altered by co-incubation of substances **1**, **2**, **4**, and satraplatin with AA and NAC (ESI Fig. S5, S7, S9, and S12). A different behaviour was observed for the fast reducing complex **3**, as the G_2/M phase arrest was attenuated by the reducing agents in A2780 cells after 48 h incubation time (G_2/M phase fraction at 15 µM, **3** alone: 61%, + AA: 47% and + NAC: 27%) compared to control (21%) (Fig. 7). These results are in line with the deactivating effect observed in the MTT assay. It is obvious that longer incubation times are required for a significant effect of the investigated Pt^{IV} complexes. As the G_2/M checkpoint is crucial for control whether DNA was correctly synthesized, the arrest is consistent with the expectation that Pt^{IV} treatment leads to DNA lesions.

PLEASE INSERT FIGURE 7 HERE

Figure 7: Impact of platinum compound **3** alone as well as co-incubated with AA (25 μM) or NAC (200 μM) on cell cycle distribution. PI staining and flow cytometry analyses were performed in A2780 and A2780cis cells after 48 h of exposure to the respective complex at the indicated concentrations. Mean percentages ± standard deviations of cells in G_0/G_1, S, and G_2/M phase of the cell cycle are shown (* $p < 0.05$; ** $p < 0.01$; $n = 3$).

Cell cycle experiments revealed that Pt^{IV} treatment of ovarian cancer cell lines has a strong impact on the distribution of cell cycle phases. A steady increase of S and G_2/M phase was observed after 24 h, turning into a G_2/M arrest after 48 h of Pt treatment. Once the cell is damaged, arrest in the G_2/M phase allows that the injured cell can either repair the damage or undergo apoptosis [32]. As the G_2/M checkpoint has the function to identify and trigger repair mechanisms, the observed G_2/M arrest suggests that Pt complexes have reached the DNA and induced severe damage. It should be kept in mind that at that point Pt^{IV} had already to be reduced, as prior experiments proved that only the Pt^{II} species interact with DNA. Concluding, intracellular reduction is highly favourable, as extracellular reduction leads to a less pronounced G_2/M arrest in A2780 cells, and as a consequence at least partly due to reduced drug accumulation.

2.6. Annexin V/PI staining

With the aim of assessing the amount of cells dying by apoptosis, annexin V/PI stained cells were counted in the flow cytometer. This method distinguishes between viable cells (AV–/PI–), early apoptosis (AV+/PI–), late apoptosis (AV+/PI+), and necrosis (AV–/PI+). For a better comparison, time and concentration ranges were chosen similarly to those of cell cycle analysis. There was mostly no change in viability of cell populations after an incubation time of 24 h in both cell lines (Fig. S13–S14, ESI). Despite the pronounced G_2/M phase arrest after 48 h for the highest concentration plotted, numbers of neither early nor late apoptotic cells were increased by the tested compounds in the cell line A2780. Therefore, it was necessary to increase the concentration to roughly 20 × IC_{50} (Fig. 8) to obtain an effect in A2780 cells. In the resistant cell line A2780cis, 20–33% late apoptotic cells were induced after 48 h by complexes **1** and **4** and 62–77% by **2**, **3**, and satraplatin at concentrations similar to those used for cell cycle analysis (Fig. 9). Thus, the investigated complexes induce apoptosis in a dose- and time-dependent manner and pronounced apoptosis was found for all complexes at the highest concentration. Our results imply that DNA damage caused by the reduction products of Pt^{IV} complexes is quite severe, leading to programmed cell death, whereas amounts of necrotic cells were similar to those in the control groups.

In order to compare the results for reduced and intact species, complex **3** was co-incubated with AA and NAC, yielding a complete loss of apoptosis induction in the cell line A2780 for both reductants, but in A2780cis only for NAC treatment (Fig S15–S16, ESI). These results corroborate the insight gained from the MTT assay, namely that the activity of this set of substances is highly dependent on reduction rates and the applied type of reducing agent.

PLEASE INSERT FIGURE 8 HERE

Figure 8: Induction of apoptosis of investigated platinum complexes **1**–**4** and reference compound satraplatin. Annexin V/PI staining and flow cytometry analyses were performed in A2780 cells after 48 h of exposure to the respective complex at indicated drug concentrations, yielding the depicted percentages of viable (AV-/PI-), early apoptotic (AV+/PI-), apoptotic (AV+/PI+), and necrotic (AV-/PI+) cells.

PLEASE INSERT FIGURE 9 HERE

Figure 9: Induction of apoptosis of investigated platinum complexes **1**–**4** and reference compound satraplatin. Annexin V/PI staining and flow cytometry analyses were performed in A2780cis cells after 48 h of exposure to the respective complex at indicated drug concentrations, yielding the depicted percentages of viable (AV-/PI-), early apoptotic (AV+/PI-), apoptotic (AV+/PI+), and necrotic (AV-/PI+) cells.

2.7. Western blotting

Western blot studies were performed in order to check for apoptosis by a method independent from the annexin V/PI assay and to identify which apoptosis pathway is involved. The change in expression of two apoptosis–related proteins (PARP; caspase 9) after treatment with complex **3** and the reference satraplatin was investigated. PARP is involved in several biological processes, most importantly in apoptosis and DNA damage response [33]. Caspase 9 is a protein centrally involved in the induction of apoptosis via the mitochondrial (intrinsic) pathway [34]. Protein levels were monitored after 24 h and 48 h incubation time in both cell lines, A2780 as well as

A2780cis, but lower concentrations of Pt^{IV} compound have to be applied in Western blotting experiments than in the annexin V/PI assay in order to obtain sufficient amounts of protein.

Both substances lead to cleavage of PARP at the highest concentration after 24 h most effectively in A2780cis cells, whereas no significant cleavage of caspase 9 was observed (Fig. 10). In A2780 cells only a negligible amount of cleaved PARP was found for both complexes, whereas a 1.5- to 2.7- fold increase of cleaved caspase 9 could be detected. Cleavage of PARP was significantly increased after 48 h, and especially for **3** at 35 μM a degradation of all investigated proteins took place in A2780cis cells. At lower concentration, caspase 9 was not altered. The results argue for the induction of apoptosis after treatment with Pt^{IV} complexes in a time- and concentration dependent manner, due to the significant cleavage of PARP. Despite the fact that no cleavage or just a minor increase of cleaved caspase 9 was detectable, which may result from the relatively long incubation times applied in these experiments (24 h and 48 h), the involvement of the intrinsic apoptosis pathway is likely for Pt^{IV} compounds. The Western blot analysis is more sensitive in examining apoptosis than the annexin V/PI staining, as already sub-IC_{50} concentrations show strong effects on the protein level, whereas effects in flow cytometric analysis were just seen for higher doses.

PLEASE INSERT FIGURE 10 HERE

Figure 10: Caspase-induced cleavage of PARP, and caspase 9 in A2780 (**A**, **B**), and A2780cis (**C**, **D**) cells after treatment with satraplatin or compound **3** at the indicated concentrations after 24 h (**A**, **C**; n = 2) and 48 h (**B**, **D**; n = 3), determined by Western blot analysis (* $p < 0.05$; ** $p < 0.01$).

2.8. Involvement of oxidative stress in Pt^{IV} cytotoxicity

Since platinum(IV) reduction involves a two-electron process, generation of radicals is quite possible. Interestingly, it has hardly been investigated whether Pt^{IV} complexes induce the formation of reactive oxygen species (ROS), whereas ROS generation has been reported in the case of cisplatin [35]. Cisplatin influences the cellular redox homeostasis and the mitochondrial redox status [36]. Nevertheless, as the generation of reactive oxygen species (ROS) during activation by reduction of Pt^{IV} is plausible and GSH and also NADH are on the one hand interacting with Pt^{IV} and on the other hand substantial in compensating cellular redox balance, a closer look on the involvement of ROS in Pt^{IV} cytotoxicity is reasonable. So far, ROS was only reported in the case of tetrachlorido platinum(IV) complexes [37].

For determination of ROS levels produced during platinum treatment, cells were stained with DCFH-DA (2',7'-dichlorofluorescein diacetate) and afterwards treated with platinum complexes for 30 min (Fig. 11). The increase of intensities of green fluorescence was measured by means of flow cytometry. The lowest concentration applied was always in the range of the concentration with the highest effect in cell cycle and annexin V/PI experiments, and due to the shorter incubation time two additional higher concentrations were chosen in order to enable comparison of these concentrations among different experiments.

In A2780 cells, a minor increase of ROS levels up to the 2.75-fold of the control was observed for compounds **3** and **4**, whereas treatment with **1**, **2**, or satraplatin did not increase the intensity of fluorescence. On the contrary, a very high production of ROS was measured for satraplatin (~11-fold), **1** (~6-fold), and **3** (~5-fold) in A2780cis cells, while the ROS levels after treatment with **2** as well as **4** remained below ca. 2.8-fold of the control.

PLEASE INSERT FIGURE 11 HERE

Figure 11: Generation of intracellular reactive oxygen species (ROS) after 30 min treatment with platinum complexes **1**–**4** and reference complex satraplatin at indicated concentrations in A2780 and A2780cis cells, detected with DCFH-DA staining and flow cytometric analysis.

Our results showed formation of ROS in both cell lines, although a stronger effect was observed in the cisplatin-resistant A2780cis cell line. Thus, Pt^{IV} compounds disturb the cellular redox homeostasis considerably. ROS formation induced by Pt^{IV} treatment may trigger additional DNA damage. It has been reported that cancer cells in advanced stages can acquire the ability to survive even under increased ROS stress [38], which may explain the higher amount of ROS in the cisplatin-resistant cell line A2780cis without increased apoptosis.

3. Conclusion

The present study deals with the impact of reductant levels on the activity of antiproliferative platinum(IV) complexes. All compounds under investigation show IC_{50} values in the low micromolar range, but strongly differ in their rate of reduction half times (from ~15 min up to >

15 h). Extracellularly added reducing agents, such as AA and NAC, have a high impact on the fast reducing complexes, whereas the slow reducing complexes are not influenced, making these complexes ideal candidates as model complexes to investigate the link between redox behaviour and antiproliferative activity. Fast reduction of Pt^{IV} results in similar cytotoxic activity as found for the corresponding Pt^{II} species, supporting the assumption that this Pt^{II} complex is the main metabolite, which is disadvantageous for this set of complexes as the Pt^{II} species is less active than the Pt^{IV} complexes. Nevertheless, plasmid interaction studies showed that reduction is mandatory for platinum(IV) substances damaging DNA. Based on our results, intracellular reduction is the preferred way of activation, as our experiments proved that extracellular reduction lead to deactivation of the complexes. Compounds with two axial carboxylato ligands are accumulated to a much higher amount than their congeners with at least one axial hydroxido moiety or the Pt^{II} compound, which correlates with the lipophilicity of these substances. Furthermore, Pt^{IV} exposure leads to a significant G_2/M arrest in A2780 cells as well as in the cisplatin resistant A2780cis cell line, resulting in apoptosis via the intrinsic apoptosis pathway. For the first time, ROS generation was experimentally determined for Pt^{IV} complexes with the ligand sphere *cis*,*trans*,*cis*-$PtN_2(OR)_2Cl_2$, underlining the importance of the role of the redox behaviour of the Pt^{IV} complexes on their cytotoxic activity (Fig. 12). Finally, the role of intracellular reduction is of major interest for future investigations.

PLEASE INSERT FIGURE 12 HERE

Figure 12: Proposed mode of action for investigated platinum(IV) complexes.

4. Experimental section

4.1. Platinum compounds

Compounds **1**–**5** and satraplatin were synthesized according to previously published procedures [9], in all complexes had a purity of > 95% proved by RP-HPLC and elemental analysis.

4.2. Rate of reduction

The reactivity of complexes **1**, **2**, **3**, **4,** and the reference compound satraplatin with cellular reductants was investigated by NMR spectroscopy. Freshly prepared stock solutions of each compound (1 mM) as well as 2 mM of ascorbic acid or 2 mM glutathione (reduced) were prepared in 20 mM of phosphate buffer (in D_2O, pD = 7.51). Reaction mixtures of compound:reductant (1:2 molar ratio) were mixed, and spectra were measured at ambient temperatures over a period of at least 24 h. The reduction was monitored by following the decrease of intensity of the signal resonating at 1.24 ppm, 2.06 ppm, 2.07 ppm, 2.06 ppm, and 2.12 ppm for **1**, **2**, **3**, **4**, and satraplatin, respectively.

4.3. Cell lines and culture conditions

Human A2780 (ovarian carcinoma) cells were kindly provided by Lloyd R. Kelland (CRC Centre for Cancer Therapeutics, Institute of Cancer Research, Sutton, U.K.) and the respective cisplatin resistant cell line A2780cis by Brigitte Marian (Institute of Cancer Research, Department of Medicine I, Medical University of Vienna, Austria). Cells were grown in 75 cm^2 culture flasks (CytoOne) as adherent monolayer cultures in complete culture medium, i.e. RPMI 1640 supplemented with 10% heat-inactivated fetal bovine serum (FBS; Invitrogen), and 4 mM L-glutamine (Sigma–Aldrich, Vienna, Austria). Cultures were maintained at 37 °C in a

humidified atmosphere containing 95% air and 5% CO_2. The resistant cell model was treated with 1 μM cisplatin (in RPMI 1640) every 3-4 passages.

4.4. Plasmid DNA interaction studies

pUC19 DNA (2686 bp) plasmid was purchased from Fermentas Life Sciences and multiplied by *E. coli* (TOP10F, Invitrogen). 500 ng of pUC19 plasmid were incubated with 50 μM of the test compound, or a mixture of 100 μM reductant (AA or GSH) and 50 μM of test compound, in a 0.1 × Tris-EDTA (TE) buffer for different time intervals (15 min up to 6 h) at 37 °C. The electrophoresis was performed in agarose (from Sigma Aldrich) gel 1% w/v in 1 × Tris-Borate-EDTA (TBE) buffer for 90 min at 80 V in 1 × TBE buffer. Gels were stained with ethidium bromide (EtBr) in 1 × TBE (0.75 μg/mL) for 20 min. Images were taken with the gel documentation system Fusion SL detection system (Vilber Lourmat, Eberhardzell, Germany).
The plasmid bands of three independent repetitions were quantified by ImageJ 1.48 software.

4.5. Cytotoxicity tests in cancer cell lines

Cytotoxicity was determined by a colorimetric microculture assay (MTT assay). For this purpose, A2780 and A2780cis cells were harvested from culture flasks by trypsinisation and seeded into 96-well microculture plates (CytoOne) in densities of 2×10^3 (A2780), 3×10^3 (A2780cis) viable cells/well, respectively. In the first 24 h, the cells were allowed to settle and resume exponential growth. Then, cells were exposed to dilutions of the test compounds in 200 μL/well RPMI 1640 medium for 96 h. At the end of exposure, drug solutions were replaced with 100 μL/well of a 6:1 mixture of RPMI 1640 medium (supplemented with 10% heat-inactivated FBS and 4 mM L-glutamine) and MTT solution (MTT reagent in phosphate-buffered saline, 5 mg/mL). After incubation for 4 h, the medium/MTT mixture was removed, and the formazan product formed by viable cells was dissolved in DMSO (150 μL/well). Optical densities at 550

nm were measured with a microplate reader (Biotek ELx808), using a reference wavelength of 690 nm to correct for unspecific absorption. The quantity of viable cells was expressed relative to untreated controls, and 50% inhibitory concentrations (IC_{50}) were calculated from concentration-effect curves by interpolation. Evaluation is based on means from at least three independent experiments, each comprising triplicates for each concentration level.

Co-incubation experiments were performed in an analogous manner, except for adding a solution of AA or NAC prior to drug treatment with an overall working solution amount of 200 µL/well. End concentrations of 25 µM for AA in both cell lines and 150 µM or 200 µM for NAC in A2780 or A2780cis cells, respectively, were applied.

4.6. Cellular accumulation

Studies on cellular accumulation were performed according to the method described previously [39]. Briefly, A2780 and A2780cis cells were seeded in twelve-well plates at densities of 3×10^5 or 2.2×10^5 per well in aliquots of 1 mL RPMI 1640 medium (see "Cell lines and culture conditions"). Accumulation experiments and corresponding adsorption/desorption controls were located on the same plate, and an additional plate included controls for cell counting. Plates were kept at 37 °C for 24 h prior to addition of the respective complex. Cells were incubated with a compound concentration of 50 µM or a mixture of 50 µM compound and 100 µM reducing agents (AA or NAC) for co-incubations experiments, respectively, for 2 h at 37 °C. Cells of the control well were counted during that time. Afterwards, the medium was removed, cells were washed three times with PBS, lyzed with 0.4 mL subboiled HNO_3 per well for 1 h at room temperature, and platinum was quantified by inductively coupled plasma mass spectrometry (ICP-MS) in aliquots of 300 µL diluted to a total volume of 8 mL. The adsorption/desorption blank data were subtracted from the data for the corresponding accumulation sample, and the

platinum content was referred to the cell number. The results are based on at least three independent experiments, each consisting of three replicates.

Lysates were diluted in 1% HNO_3, and determination of platinum was carried out with an ICP-quadrupole MS Agilent 7500ce instrument (Agilent Technologies, Waldbronn, Germany). The ICP-MS instrument was equipped with a CETAX ASX-520 autosampler (Nebraska, USA) and a MicroMist nebulizer operating at a sample uptake rate of approx. 0.25 mL per min. Platinum and rhenium standards were obtained from CPI International (Amsterdam, The Netherlands), with rhenium serving as internal standard. The instrument was tuned on a daily basis in order to achieve maximum sensitivity. Quantification was done using the isotopes ^{185}Re and ^{195}Pt with a dwell time of 0.3 s and 10 replicates. The instrument was equipped with nickel cones and was operated at an RF power of 1550 W, with argon as plasma gas (15 L/min) as well as carrier gas (1.10 L/min). The Agilent MassHunter software package (Workstation Software, Version B.01.01, 2012) was used for data processing. As unspecific binding to cell culture plastic ware may occur especially in case of lipophilic compounds, results were corrected for platinum levels of a blank well containing no cells.

4.7. Cell cycle studies

For this assay, A2780 and A2780cis cells were harvested by trypsinisation, and 1×10^5 cells for 24 h incubation and 5×10^4 cells for 48 h incubation were seeded into 24-well plates (1 mL/well). In the first 24 h, the cells were allowed to settle and resume exponential growth. Thereafter, the medium was removed, and 0.5 mL/well of stocks of RPMI 1640 medium, ascorbic acid (50 µM, end conc. 25 µM) or NAC (400 µM, end conc. 200 µM) were added. Furthermore, stocks of the test compounds in RPMI 1640 were diluted, and 0.5 mL/well were added to the plate. After continuous exposure for 24 h and 48 h (in the incubator at 37 °C and

under 5% CO_2), the cells were washed with PBS and trypsinised. Trypsinisation was stopped by RPMI 1640, the cells were centrifuged (300 g, 3 min), and the supernatant was discarded. The cells were washed with PBS and resuspended in 600 µL PI/HSF buffer (0.1% v/v Triton X-100, 0.1% w/v sodium citrate, in PBS) containing 50 µg/mL propidium iodide (PI). After incubation overnight at 4 °C in the dark, 5×10^3 cells were measured by flow cytometry with a Millipore guava easy cyte 8HT instrument. Data were evaluated by FlowJo software (Tree Star) using Dean Jett Fox algorithms. Tests were repeated in at least three independent experiments.

4.8. Annexin V/PI assay (apoptosis)

Cell death induction was analysed by flow cytometry using FITC-conjugated annexin V (BioVision, USA) and propidium iodide (PI, Fluka) staining. A2780 and A2780cis cells were seeded into 24-well plates (Starlab, CytoOne) in densities of 1×10^5 cells for 24 h, and 5×10^4 cells for 48 h incubation time in 1 mL/well complete medium (RPMI 1640) and allowed to settle for 24 h. Thereafter, the medium was removed, and 0.5 mL of RPMI 1640 or stock solutions of AA or NAC in RPMI 1640 were added, followed by the exposure to compounds in different concentrations for 24 h and 48 h (37 °C, 5% CO_2). After incubation, the cells were gently trypsinised and harvested, centrifuged (300 g, 3 min), and the supernatant was discarded. The cells were resuspended with FITC-conjugated annexin V (0.25 µg/mL) in binding buffer (10 mM HEPES/NaOH pH 7.4, 140 mM NaCl, 2.5 mM $CaCl_2$) and incubated at 37 °C for 15 min. PI (1 µg/mL) was added shortly before measurement. Stained cells were analysed with a Millipore guava easy cyte 8HT flow cytometer using InCyte software. The resulting dot plots were quantified by FlowJo software (TreeStar). At least three independent experiments were conducted for 5×10^3 cells per analysis.

4.9. Western blotting

After 24 h or 48 h of drug exposure, total cell lysates were prepared by lysis with RIPA buffer including protease and phosphatase inhibitor cocktails (Sigma Aldrich). Identical amounts of total proteins were seperated by SDS−PAGE, and electrophoretically transferred onto a PVDF membrane by using a semi-dry blotter (Peqlab, Erlangen, Germany). The membrane was blocked with 5% w/v nonfat dry milk in Tris-buffered saline/Tween 20 buffer for 1 h at room temperature. The anti-poly(ADP-ribosyl)polymerase (PARP), cleaved PARP, caspase 9, and cleaved caspase 9 antibodies from the apoptosis sampler kit (Cell Signaling Technology, Beverly, MA) were used in a 1:1000 dilution and the anti-*β*-actin monoclonal rabbit AC-15 antibody (Sigma) in a 1:2000 dilution and incubated according to the manufacturer's instructions. Anti-*β*-actin was used as loading control. Secondary antibodies were appropriately diluted and incubated for 1 h at room temperature. Horseradish peroxidase-coupled secondary antibodies were used at working dilutions of 1:10000 and detected by chemiluminescence using the Pierce SuperSignal chemiluminescence substrate (Thermo Fisher Scientific, Inc., Rockford, IL) and the Fusion SL chemiluminescence detection system (Vilber Lourmat, Eberhardzell, Germany). Protein expressions were quantified by ImageJ 1.48 software for at least two independent repetitions, corrected to β-actin levels and normalized to control.

4.10. DCFH-DA assay

For the fluorimetric analysis of reactive oxygen species (ROS), A2780 and A2780cis cells were washed with PBS and trypsinised. Trypsinisation was stopped by RPMI 1640, then 8×10^5 cells/mL were transferred in a 15 mL tube and centrifuged (300 g, 3 min). The supernatant was discarded, and the cells were washed with PBS and resuspended in Hank's Balanced Salt Solution supplemented with 1% heat-inactivated FBS. The cell suspension was stained for 30

min at 37 °C with 1 μM DCFH-DA (2',7'-dichlorofluorescein diacetate). 8×10^4 cells/well were transferred into 96-well plates and treated with the test substance at different concentrations for 30 min at 37 °C, 5% CO_2. 500 μM freshly prepared H_2O_2 solution was used as a positive control and added 10 min before measurement. The generated ROS activity within the cells was measured by flow cytometry on a guava easy cyte 8HT device (Millipore). The resulting histograms of green fluorescence were quantified by FlowJo software (Tree Star). Green fluorescence intensity is the ratio between fluorescence of the drug-treated sample and that of the untreated control.

4.11. Statistical analysis

Results were expressed as the mean ± SD. Statistical calculations were performed using GraphPad Prism 6. The criterion for statistical significance was taken as $p < 0.05$ or $p < 0.01$, achieved by two way ANOVA, whenever indicated by * or **, respectively.

Conflict of interests

The authors declare no conflict of interests.

Acknowledgement

V.P. wants to thank S. Theiner, M. Klose and R. Bugl for ICP-MS measurements and V. Somoza for providing the Fusion SL detection system. The authors are indebted to the FFG – Austrian Research Promotion Agency (811591), the Johanna Mahlke née Obermann Foundation for Cancer Research, and the COST action (CM1105).

[1] N. J. Wheate, S. Walker, G. E. Craig, and R. Oun, *Dalton Trans.,* 2010, 39, 8113–8127.

[2] N. Muhammad and Z. Guo, *Curr. Opin. Chem. Biol.*, 2014, 19, 144–153.

[3] N. Graf and S. J. Lippard, *Adv. Drug Delievery Rev.*, 2012, 64, 993–1004.

[4] J. L. Carr, M. D. Tingle and M. J. McKeage, *Cancer Chemother. Pharmacol.*, 2002, 50, 9–15.

[5] W. Zhong, Q. Zhang, Y. Yan, S. Yue, B. Zhang, and W. Tang, *J. Inorg. Biochem.*, 1997, 3, 159–164.

[6] M. R. Reithofer, A. K. Bytzek, S. M. Valiahdi, C. R. Kowol, M. Groessl, C. G. Hartinger, M. A. Jakupec, M. Galanski, and B. K. Keppler, *J. Inorg. Biochem.*, 2011, 105, 46–51.

[7] J. A. Platts, G. Ermondi, G. Caron, M. Ravera, E. Gabano, L. Gaviglio, G. Pelosi, and D. Osella, *J. Biol. Inorg. Chem.*, 2011, 16, 361–372.

[8] J. Z. Zhang, E. Wexselblatt, T. W. Hambley, and D. Gibson, *Chem. Commun.*, 2012, 48, 847–849.

[9] V. Pichler, S. Göschl, S. M. Meier, A. Roller, M. A. Jakupec, M. Galanski, and B. K. Keppler, *Inorg. Chem.*, 2013, 52, 8151–8162.

[10] H. P. Varbanov, S. M. Valiahdi, C. R. Kowol, M. A. Jakupec, M. Galanski, and B. K. Keppler, *Dalton Trans.*, 2012, 41, 14404–14415.

[11] S. Huo, J. Dong, S. Shen, Y. Ren, C. Song, J. Xu, and T. Shi, *Dalton Trans.*, 2014, 43, 15328–15336.

[12] E. Petruzzella, N. Margiotta, M. Ravera, and G. Natile, *Inorg. Chem.*, 2013, 52, 2393–2403.

[13] J. J. Wilson and S. J. Lippard, *Chem. Rev.*, 2014, 114, 4470–4495.

[14] C. F. Chin, Q. Tian, M. I. Setyawati, W. Fang, E. S. Q. Tan, D. T. Leong, and W. H. Ang, *J. Med. Chem.*, 2012, 55, 7571–7582.

[15] M. Ravera, E. Gabano, G. Pelosi, F. Fregonese, S. Tinello, and D. Osella, *Inorg. Chem.*, 2014, 53, 9326–9335.

[16] J. M. Perez, M. Camazón, A. Alvarez-Valdes, A. G. Quiroga, L. R. Kelland, C. Alonso, and M. C. Navarro-Ranninger, *Chem. Biol. Interact.*, 1999, 117, 99–115.

[17] M. Galanski and B. K. Keppler, *Inorg. Chim. Acta*, 2000, 300, 783–789.

[18] C. F. O'Neill, B. Koberle, J. R. W. Masters, and L. R. Kelland, *Br. J. Cancer*, 1999, 81, 1294–1303.

[19] M. Kalimutho, A. Minutolo, S. Grelli, G. Federici, and S. Bernardini, *Acta Pharmacol. Sin.*, 2011, 32, 1387–1396.

[20] M. G. Ormerod, R. M. Orr, C. F. O'Neill, T. Chwalinski, J. C. Titley, L. R. Kelland, and K. R. Harrap, *Br. J. Cancer*, 1996, 74, 1935–1943.

[21] M. Jiang, C. Y. Wang, S. Huang, T. Yang, and Z. Dong, *Am. J. Physiol. Renal. Physiol.*, 2009, 296, F983–993.

[22] H. Taube, *Chem. Rev.*, 1952, 50, 69–126.

[23] C. K. J. Chen, J. Z. Zhang, J. B. Aitken, and T. W. Hambley, *J. Med. Chem.*, 2013, 56, 8757–8764.

[24] C. Bartel, A. K. Bytzek, Y. Y. Scaffidi-Domianello, G. Grabmann, M. A. Jakupec, C. G. Hartinger, M. Galanski, and B. K. Keppler, *J. Biol. Inorg. Chem.*, 2012, 17, 465–474.

[25] M. S. Davies, S. J. Berners-Price, and T. W. Hambley, *Inorg. Chem.*, 2000, 39, 5603–5613.

[26] Y. Zou, B. Van Houten, and N. Farrell, *Biochemistry*, 1993, 32, 9632–9638.

[27] J. Banfic, M. S. Adib-Razavi, M. Galanski, and B. K. Keppler, *Z. Anorg. Allg. Chem.*, 2013, 8–9, 1613–20.

[28] A. Nemirovski, Y. Kasherman, Y. Tzaraf, and D. Gibson, *J. Med. Chem.*, 2007, 50, 5554–5556.

[29] G. N. Kaluderovic, H. Kommera, S. Schwieger, A. Paethanom, M. Kunze, H. Schmidt, R. Paschke, and D. Steinborn, *Dalton Trans.*, 2009, 10720–10726.

[30] B. C. Behrens, T. C. Hamilton, H. Masuda, K. R. Grotzinger, J. Whang-Peng, K. G. Louie, T. Knutsen, W. M. McKoy, R. Young, and R. F. Ozols, *Cancer Res.*, 1987, 47, 414–418.

[31] V. Pichler, P. Heffeter, S. M. Valiahdi, C. R. Kowol, A. Egger, W. Berger, M. A. Jakupec, M. Galanski, and B. K. Keppler, *J. Med. Chem.,* 2012, 55, 11052–11061.

[32] R. S. DiPaola, *Clin. Cancer Res.*, 2002, 8, 3311–3314.

[33] M. Isabelle, X. Moreel, J.-P. Gangé, M. Rouleau, C. Ethier, P. Gagné, M. J. Hendzel, and G. G. Poirier, *Proteome Science*, 2010, 8, 1–22.

[34] D. R. McIlwain, T. Berger, and T. W. Mak, *Cold Spring Harb. Perspect. Biol.*, 2013, 5, 1–28.

[35] H. Pelicano, D. Carney, and P. Huang, *Drug Res. Updates*, 2004, 7, 97–100.

[36] U. Jungwirth, C. R. Kowol, B. K. Keppler, C. G. Hartinger, W. Berger, and P. Heffeter, *Antioxidants & Redox. Signaling*, 2011, 15, 1085–1127.

[37] G. N. Kaluderovi`c, S. A. Mijatovi´c, B. B. Zmejkovski, M. Z. Bulatovi´c, S. Gómez-Ruiz, M. K. Moji´c, D. Steinborn, D. M. Miljkovi´c, H. Schmidt, S. D. Stosi´c-Grujici´c, T. J. Sabo, and D. D. Maksimovi´c-Ivani´c, *Metallomics*, 2012, 4, 979–987.

[38] D. Trachootham, J. Alexandre, and P. Huang, *Nature Rev. Drug Discovery*, 2009, 8, 579–591.

[39] A. Egger, C. Rappel, M. A. Jakupec, C. G. Hartinger, P. Heffeter, and B. K. Keppler, *J. Anal. At. Spectrom.*, 2009, 24, 51–61.

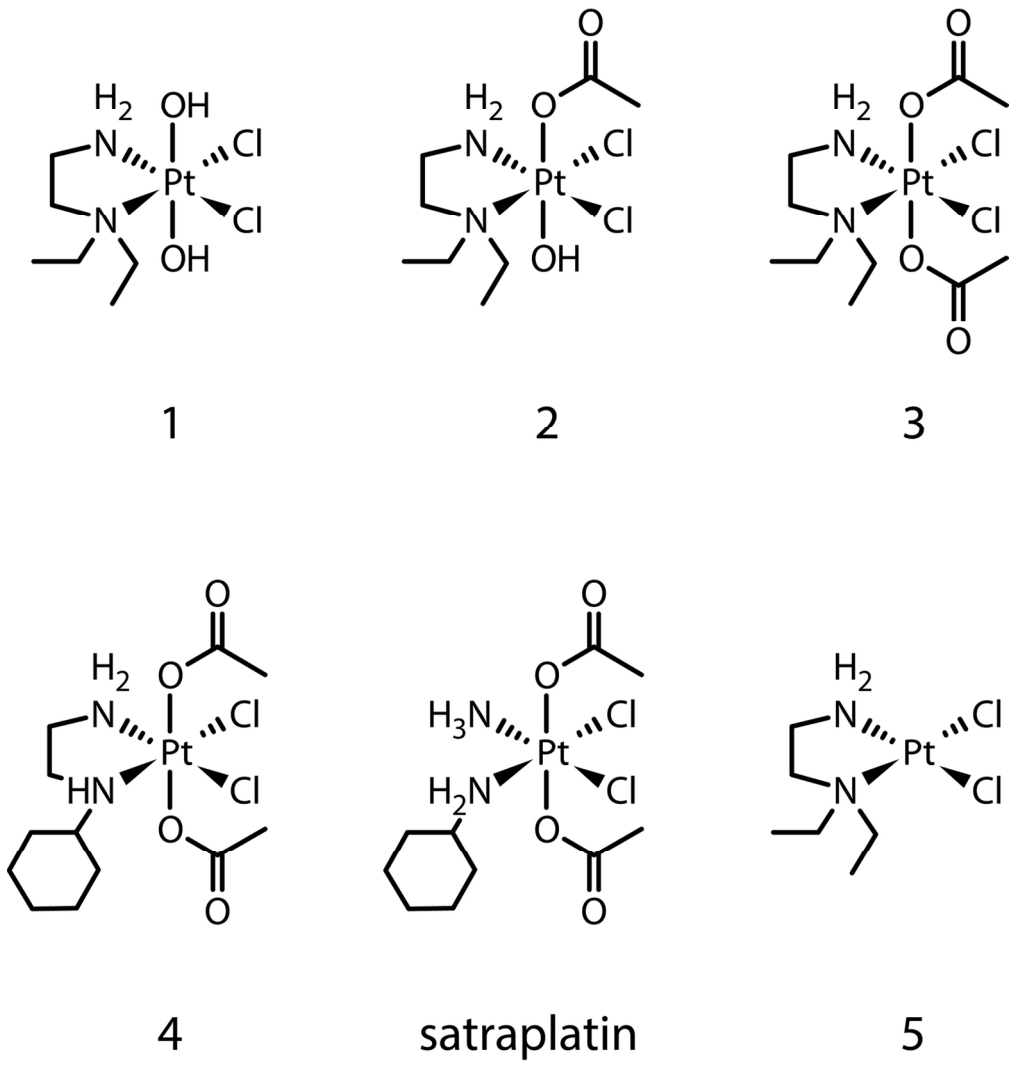

Figure 1
135x143mm (300 x 300 DPI)

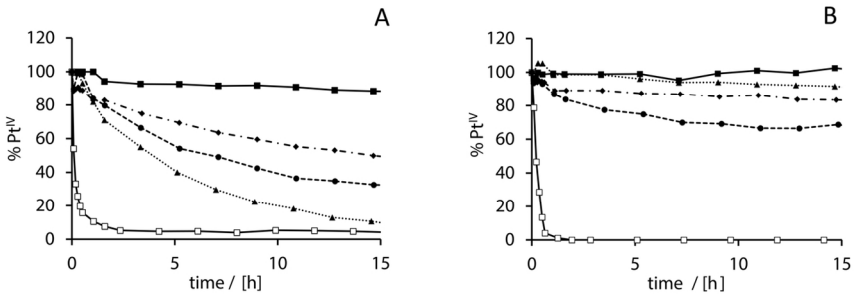

Figure 2
135x43mm (300 x 300 DPI)

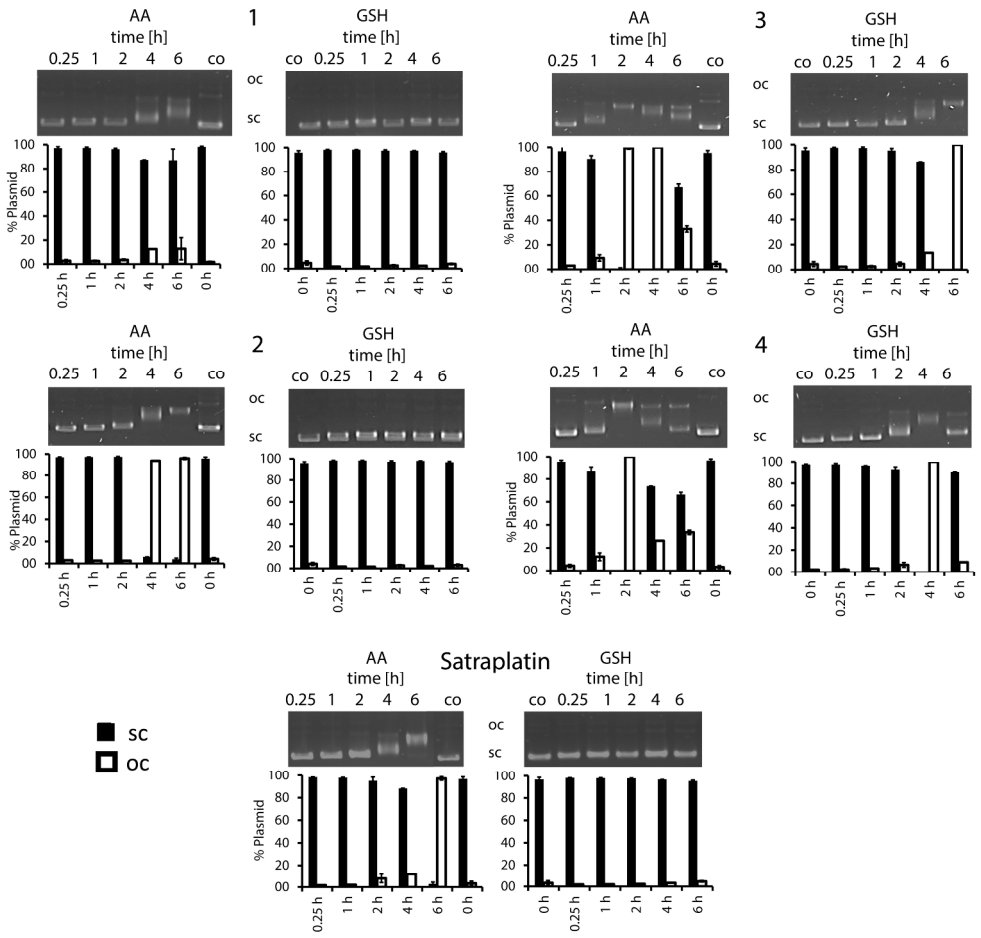

Figure 3
254x254mm (300 x 300 DPI)

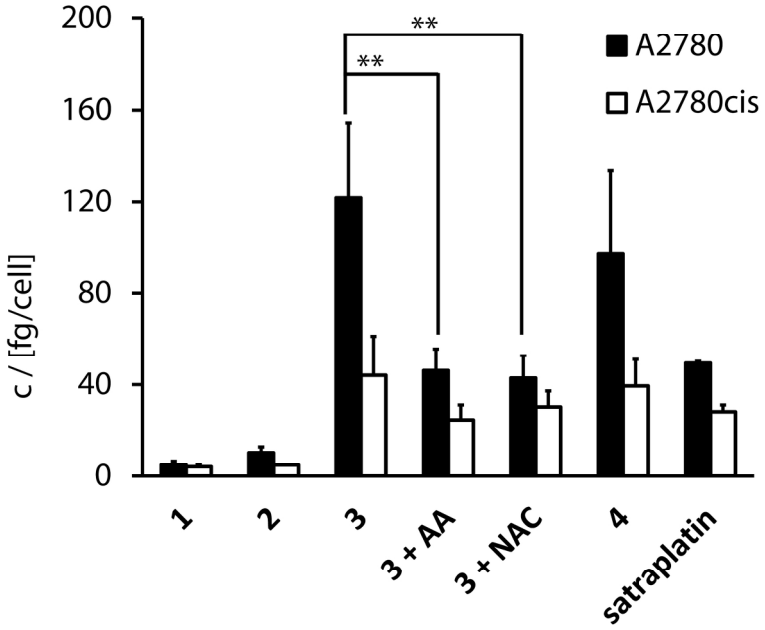

Figure 4
190x142mm (300 x 300 DPI)

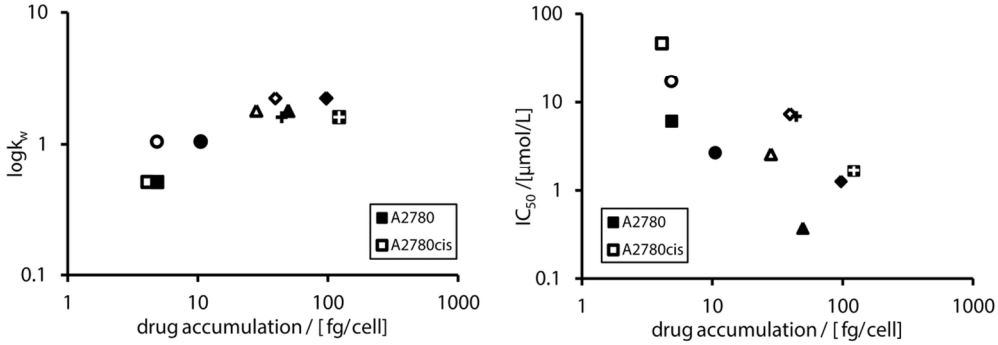

Figure 5
109x40mm (300 x 300 DPI)

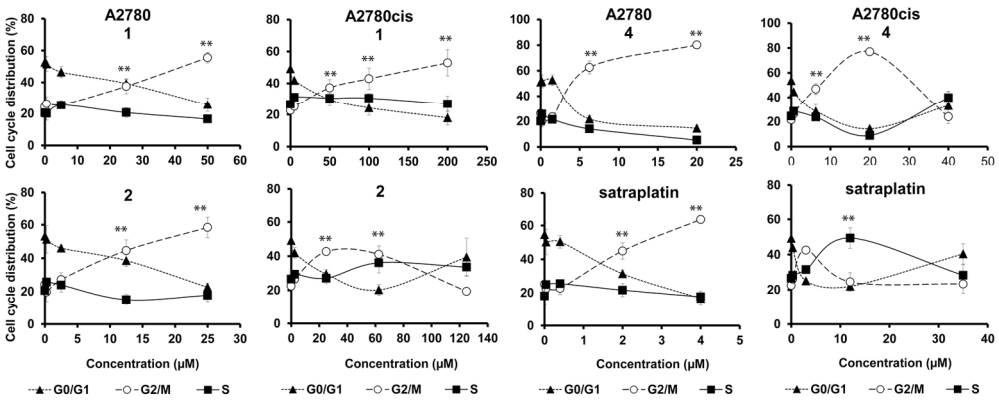

Figure 6
160x64mm (300 x 300 DPI)

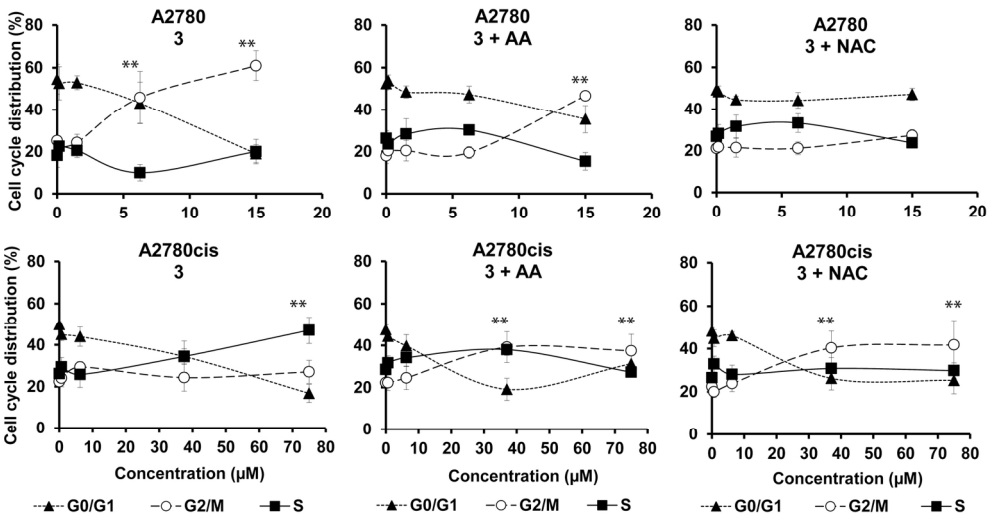

Figure 7
160x85mm (300 x 300 DPI)

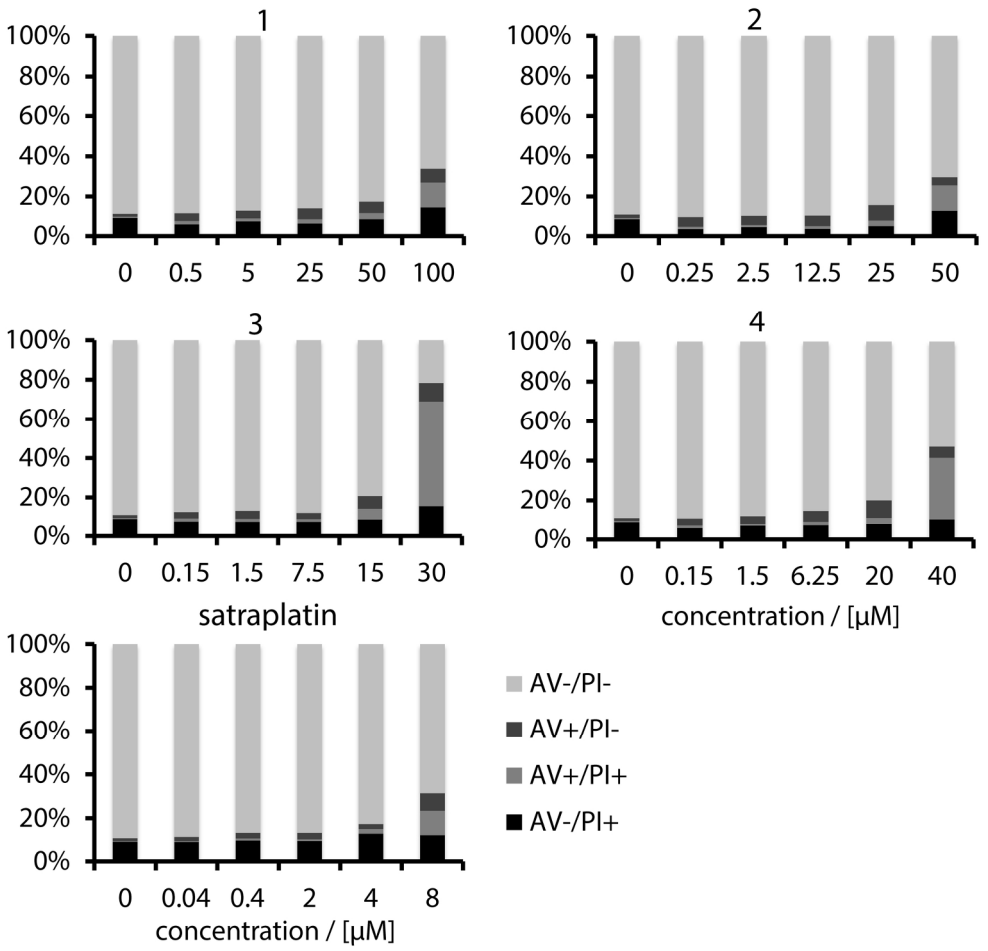

Figure 8
190x180mm (300 x 300 DPI)

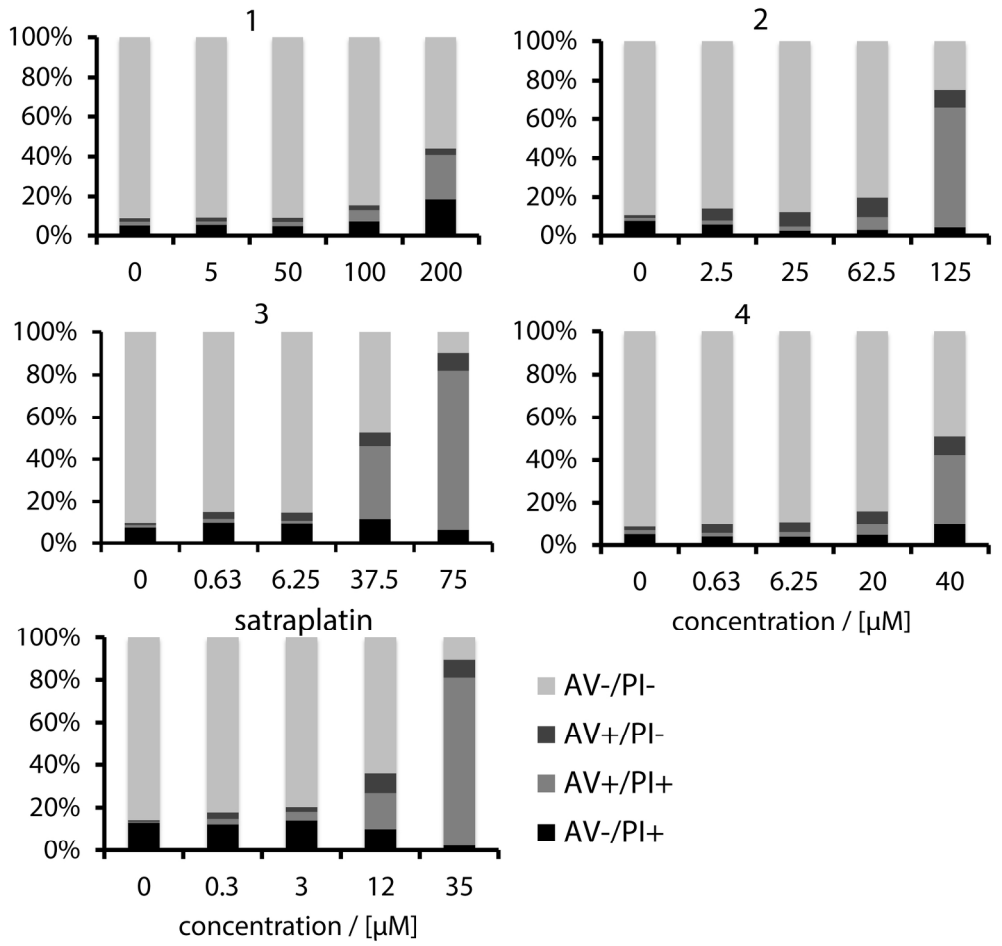

Figure 9
190x180mm (300 x 300 DPI)

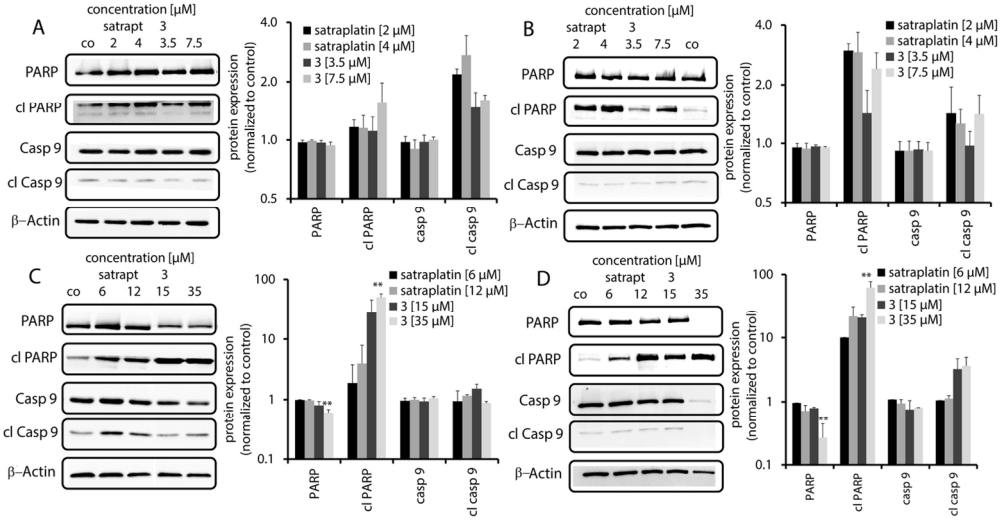

Figure 10
132x69mm (300 x 300 DPI)

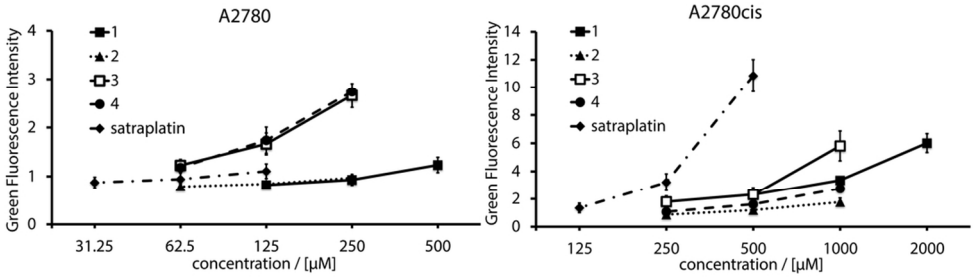

Figure 11
101x30mm (300 x 300 DPI)

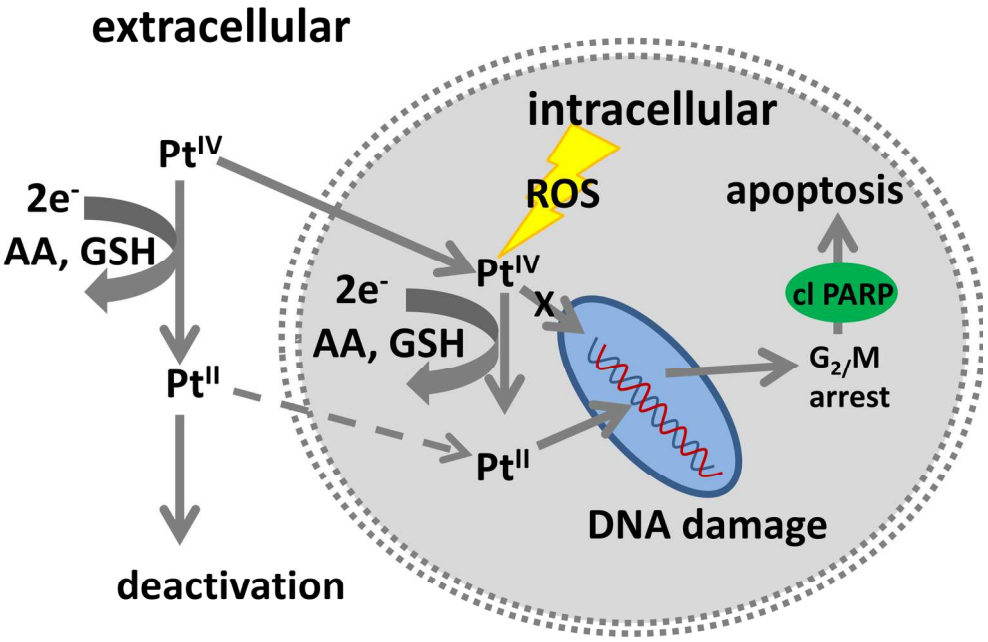

Figure 12
190x142mm (300 x 300 DPI)